

## Binding of CO to structural models of the bimetallic subunit at the A-cluster of acetyl coenzyme A synthase/CO dehydrogenase†

Todd C. Harrop,<sup>a</sup> Marilyn M. Olmstead<sup>b</sup> and Pradip K. Mascharak<sup>\*a</sup>

<sup>a</sup> Department of Chemistry and Biochemistry, University of California, Santa Cruz, CA 95064, USA

<sup>b</sup> Department of Chemistry, University of California, Davis, CA 95616, USA

Received (in West Lafayette, IN, USA) 14th April 2004, Accepted 3rd June 2004

First published as an Advance Article on the web 12th July 2004

**Trinuclear Ni–Cu–Ni and Ni–Ni–Ni complexes derived from an Ni(II)–dicarboxamido–dithiolato metallosynthon exhibit redox behavior and CO binding properties similar to those of the A-cluster in acetyl coenzyme A synthase/CO dehydrogenase (ACS/CODH).**

Acetyl coenzyme A synthase/carbon monoxide dehydrogenase (ACS/CODH) is a bifunctional enzyme present in a number of acetogenic, methanogenic, and sulfate-reducing bacteria.<sup>1</sup> The enzyme catalyzes two very important biological processes namely, the reduction of atmospheric CO<sub>2</sub> to CO (CODH) and the synthesis of acetyl coenzyme A (ACS) from CO, CH<sub>3</sub> from a corrinoid iron-sulfur protein, and the thiol coenzyme A. CODH activity occurs in the C cluster and comprises a NiFe<sub>3</sub>S<sub>4</sub> cubane unit for reversible CO<sub>2</sub> reduction. ACS activity occurs in the A cluster, the structure of which has only recently been determined by X-ray diffraction studies.<sup>2,3</sup> The structure(s) of ACS/CODH from *Moorella thermoacetica* revealed an unprecedented structure with three different metallic units linked to each other through bridging Cys–S residues comprising the active site.<sup>2,3</sup> In these structure(s) an Fe<sub>4</sub>S<sub>4</sub> cubane is bridged *via* Cys–S to a bimetallic metal cluster (Fig. 1). This bimetallic cluster contains a four-coordinate Ni, Cu, or Zn as the proximal metal (to the Fe<sub>4</sub>S<sub>4</sub> cluster; designated M<sub>p</sub>), which in turn is bridged through two Cys–S residues to a terminal square-planar Ni(II) (Ni<sub>d</sub>, distal to Fe<sub>4</sub>S<sub>4</sub>) ligated to two deprotonated carboxamido nitrogens from the peptide backbone. In addition to the three bridging Cys–S moieties around M<sub>p</sub> a fourth, still unidentified, non-protein ligand is also bound to complete the coordination sphere. Although the initial ACS structure contained Cu at the M<sub>p</sub> site, more evidence has pointed towards Ni as being the metal responsible for the ACS activity.<sup>4</sup> Our continued interest in metal complexes with mixed carboxamido–N/thiolato–S donor sets<sup>5</sup> has prompted us to explore similar complexes with Ni in hopes of understanding some of the intrinsic properties of the unique site in ACS. In this communication, we report the synthesis of sulfur-bridged trinuclear species utilizing the Ni(II)–dicarboxamido–dithiolato complex [Ni(NpPepS)]<sup>2–</sup> as the metallosynthon for the construction of higher nuclearity complexes.<sup>6</sup> Initial reactivity studies indicate that the central Ni site in these trinuclear complexes mimics for the first time several properties associated with the M<sub>p</sub> site including: (i) oscillating coordination geometry, (ii) removal with 1,10-phenanthroline (phen) indicating a labile Ni, (iii) reduction to Ni(I) state (NiFeC EPR signal), and (iv) binding of CO.

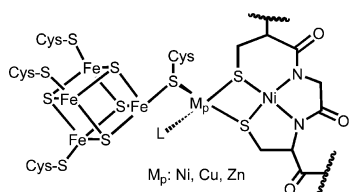


**Fig. 1** Schematic of the A-cluster of ACS/CODH from *Moorella thermoacetica*. M<sub>p</sub> has been identified as Ni, Cu, or Zn; L is an unknown ligand.

† Electronic supplementary information (ESI) available: Experimental details. See <http://www.rsc.org/suppdata/cc/b4/b405572c/>

Our approach has been similar to other current modeling efforts in which incorporation of the Fe<sub>4</sub>S<sub>4</sub> cluster is ignored and the design focuses on the bimetallic S-bridged Ni<sub>d</sub>–M<sub>p</sub> unit (proposed site(s) for acetyl CoA assembly).<sup>7</sup> In this regard, we took advantage of the monomeric dicarboxamido–dithiolato Ni(II) complex namely (Et<sub>4</sub>N)<sub>2</sub>[Ni(NpPepS)] (**1**) synthesized earlier in this lab as an appropriate model for the M<sub>d</sub> site and utilized this unit as a metalloligand synthon for bridging other metal or metal–ligand units.<sup>6</sup>

Reaction of CuCl or [Cu(MeCN)<sub>4</sub>]PF<sub>6</sub> with a solution of [Ni(NpPepS)]<sup>2–</sup> in DMF/MeCN (1/1) afforded the structurally characterized trinuclear species (Et<sub>4</sub>N)<sub>3</sub>[Cu{Ni(NpPepS)}<sub>2</sub>] (**2**) with two NiN<sub>2</sub>S<sub>2</sub> units bridged to a Cu(I) ion through thiolato–S in a distorted tetrahedral geometry (Fig. 2).<sup>‡</sup> This trimeric complex forms regardless of stoichiometry of the reagents. Unlike the reactions reported by Riordan<sup>7a</sup> and Rauchfuss,<sup>7b</sup> both thiolate moieties within the same NpPepS<sup>4–</sup> ligand frame only bind to one and not two different Cu(I) ions. The unique folding and steric demands imposed by the NpPepS<sup>4–</sup> ligand may play a role in formation of this trinuclear species. This complex structurally mimics the Cu(I) structure of ACS/CODH in many regards, the only difference being one extra metal-sulfur donor coordinated to the Cu(I) center. No reaction was observed between **2** and CO(g) under a variety of conditions<sup>7b</sup> and unlike previous work,<sup>7a</sup> no rupture of Cu–S bond was noted. Also, the Cu(I) center in **2** is

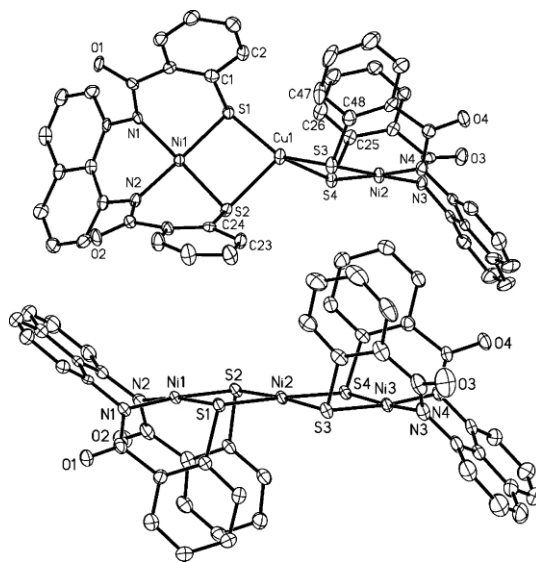


**Fig. 2** Thermal ellipsoid plot (50 % probability) of the anions of **2** (top) and **3** (bottom) with the atom-labeling scheme. H atoms are omitted for the sake of clarity. Selected bond distances for **2** (Å): Ni(1)–Cu(1), 3.259(9); Ni(1)–N(1), 1.905(4); Ni(1)–S(1), 2.1858(14); Cu(1)–S(1), 2.2824(13); Cu(1)–S(2), 2.4215(14). Selected bond angles for **2** (°): N(1)–Ni(1)–N(2), 88.67(16); N(2)–Ni(1)–S(1), 176.91(13); S(1)–Cu(1)–S(3), 144.78(5); S(3)–Cu(1)–S(4), 85.37(5). Selected bond distances for **3** (Å): Ni(1)–Ni(2), 3.2410(7); Ni(1)–N(1), 1.884(3); Ni(1)–S(1), 2.1820(11); Ni(2)–S(1), 2.2331(10). Selected bond angles for **3** (°): N(2)–Ni(1)–N(1), 89.16(14); N(2)–Ni(1)–S(1), 170.96(10); S(3)–Ni(2)–S(2), 175.61(4); S(2)–Ni(2)–S(4), 96.07(4).

removable by treatment with neocuproine but not phenanthroline.<sup>4a</sup>

The failure of the Ni–Cu–Ni models to bind CO prompted us to synthesize the analogous Ni–Ni–Ni complex. The reaction of an MeCN solution of 2 equivalents of **1** with 1 equivalent of  $[\text{NiCl}_4]^{2-}$  afforded the black-red trimeric complex  $[\text{Ni}\{\text{Ni}(\text{NpPepS})\}_2]^{2-}$  (**3**), which was shown crystallographically to adopt the ‘slant chair’ structure with an extended plane arising from the three coplanar  $\text{Ni}^{2+}$  centers (Fig. 2).<sup>†</sup> Since the central Ni (designated  $\text{Ni}_C$ ) in this species serves as a good structural model of the  $(\text{Cys-S})_3 \text{Ni}_p$  site in ACS, we were curious to study its reactivity. When the highly insoluble **3** was stirred in DMF, the initial slurry turned homogeneous and the structure of the solid isolated from the bright red solution revealed two DMF molecules coordinated to  $\text{Ni}_C$  in *cis* fashion along with structural rearrangement of the two terminal  $[\text{Ni}(\text{NpPepS})]^{2-}$  units forming  $(\text{Et}_4\text{N})_2[\text{Ni}(\text{DMF})_2\{\text{Ni}(\text{NpPepS})\}_2]$  (**4**) (Fig. 3).<sup>†</sup> Comparison of the metric parameters of the octahedral  $\text{Ni}_C$  in **4** with the square-planar  $\text{Ni}_C$  in **3** reveals significant increases in the Ni–S and Ni–Ni bond distances upon expansion of the coordination sphere. It is interesting to note that the  $\text{Ni}_C$  center in **3** expands its coordination sphere much like the  $\text{Ni}_p$  center in ACS.<sup>3</sup>

The mechanism of acetyl coenzyme A assembly at the ACS site and the nature of the intermediates involved remain elusive at this time. The enzyme has been proposed to exist in two forms: oxidized ( $\text{A}_{\text{ox}}$ ) and one electron reduced with bound CO ( $\text{A}_{\text{red}}\text{-CO}$ ).<sup>1</sup> Upon reductive carbonylation, a characteristic EPR spectrum (NiFeC signal) is observed and the  $\nu_{\text{CO}}$  band at  $1996 \text{ cm}^{-1}$  indicates the formation of a terminal Ni(i)–CO species.<sup>1,8</sup> Titration of the enzyme with phenanthroline results in loss of the NiFeC EPR signal along with its ACS activity.<sup>1</sup> Reconstitution of phenanthroline-treated ACS with  $\text{NiCl}_2$  replenishes both the activity and the EPR signal. Complex **4** exhibits some of these characteristics of the ACS active site. For example, when **4** is reduced with  $\text{Na}_2\text{S}_2\text{O}_4$  or  $\text{NaBH}_4$  in DMF, the resulting **4**<sub>red</sub> exhibits a strong EPR signal with  $g = 2.33$  and  $2.09$  (Fig. S1)<sup>†</sup> consistent with a Ni(i) center in a tetrahedral  $\text{S}_4$  coordination sphere.<sup>9</sup> Passage of CO through the solution of **4**<sub>red</sub> in DMF affords the CO-adduct that exhibits  $\nu_{\text{CO}}$  at  $1960 \text{ cm}^{-1}$  (Fig. S2)<sup>†</sup> consistent with a terminal Ni(i)–CO unit. No reaction with CO is observed with either a solution of **4** in DMF or a solution of the monomeric complex **1** in DMF under similar reducing conditions. Since the Cu(i) trimer **2** shows no reduction up to  $-1.8 \text{ V}$  (vs. saturated calomel electrode) in DMF, it is clear that the terminal  $\text{NiN}_2\text{S}_2$  units are not reduced under the reaction conditions mentioned above. Collectively, these results demonstrate that the  $\text{Ni}_C$  in **4** (and also in **3**) is the site of reduction and CO binding. This in turn supports the notion that the metallosulfur ligated  $\text{Ni}_p$  in ACS is most possibly the site of reduction and CO binding. Furthermore, phenanthroline removes  $\text{Ni}_C$  in **4**, as in ACS, affording monomeric **1** and  $[\text{Ni}(\text{phen})_3]^{2+}$  (as followed by its electronic absorption spectrum in DMF; Fig. S3).<sup>†</sup> Even addition of up to 100 equivalents of phenanthroline to **1** or **4** results in no

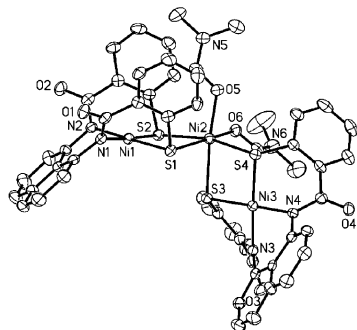


**Fig. 3** Thermal ellipsoid plot (50% probability) of the anion of **4**. H atoms omitted for the sake of clarity. Selected bond distances (Å): Ni(1)–Ni(2), 3.374(3); Ni(1)–N(1), 1.898(3); Ni(1)–S(1), 2.1828(12); Ni(2)–S(1), 2.4877(13); Ni(2)–S(3), 2.4495(12). Selected bond angles (°): N(2)–Ni(1)–N(1), 87.99(15); N(2)–Ni(1)–S(1), 177.93(11); O(5)–Ni(2)–O(6), 85.60(12); S(2)–Ni(2)–S(4), 166.05(5).

further change in the electronic absorption spectrum suggesting that the  $\text{Ni}_d$  is not responsible for the ACS activity. The reactions of the trimeric species **3** and **4** are schematically summarized in Scheme S1.<sup>†</sup>

In summary, we report a series of structurally characterized sulfur bridged trimetallic complexes bearing close structural and spectroscopic resemblance to the proposed substrate binding bimetallic subunit in the A-cluster of ACS/CODH. To our knowledge, these are the first examples of complexes that mimic many of the characteristics associated with the ACS site. The consistent lack of reactivity of the Cu(i) complex **2** and other similar Cu(i) species<sup>7</sup> strongly suggests that Cu(i) may not be the catalytically active metal at the  $\text{M}_p$  site of ACS. In contrast, the chemical behavior of the central Ni ion in **3** lends further support in favor of Ni at  $\text{M}_p$  site in catalytically active ACS.

Financial support from the NIH grant GM61636 is gratefully acknowledged. T.C.H. received support from the NIH IMSD grant GM58903.

## Notes and references

<sup>†</sup> Crystal data for **2**·DMF,  $\text{Ni}_2\text{CuC}_{75}\text{H}_{95}\text{N}_8\text{O}_5\text{S}_4$ ,  $M = 1497.79$ , monoclinic, space group  $P2_1/c$ ,  $a = 20.4393(17) \text{ \AA}$ ,  $b = 19.5132(18) \text{ \AA}$ ,  $c = 19.661(2) \text{ \AA}$ ,  $\alpha = 90^\circ$ ,  $\beta = 116.526(3)^\circ$ ,  $\gamma = 90^\circ$ ,  $V = 7016.1(11) \text{ \AA}^3$ ,  $Z = 4$ ,  $D_c = 1.418 \text{ Mg m}^{-3}$ ,  $\mu(\text{Mo-K}\alpha) = 1.008 \text{ mm}^{-1}$ ,  $T = 93(2)$ , Crystal size,  $0.16 \times 0.13 \times 0.02 \text{ mm}^3$ , 47282 reflections measured, 13298 unique ( $R_{\text{int}} = 0.113$ ), final  $R_1 = 0.0523$ ,  $wR_2 = 0.1106$ . Diffraction data were collected at 93 K on a Bruker SMART 1000 CCD diffractometer. Solution and refinement were solved by direct methods (standard SHELXS-97 package).

For **3**·DMF,  $\text{Ni}_3\text{C}_{67}\text{H}_{74}\text{N}_7\text{O}_5\text{S}_4$ ,  $M = 1361.70$ , monoclinic, space group  $P2_1/c$ ,  $a = 18.6353(15) \text{ \AA}$ ,  $b = 20.2119(17) \text{ \AA}$ ,  $c = 17.3241(14) \text{ \AA}$ ,  $\alpha = 90^\circ$ ,  $\beta = 110.887(3)^\circ$ ,  $\gamma = 90^\circ$ ,  $V = 6096.4(9) \text{ \AA}^3$ ,  $Z = 4$ ,  $D_c = 1.484 \text{ Mg m}^{-3}$ ,  $\mu(\text{Mo-K}\alpha) = 1.112 \text{ mm}^{-1}$ ,  $T = 90(2)$ , crystal size,  $0.20 \times 0.16 \times 0.09 \text{ mm}^3$ , 52356 reflections measured, 13981 unique ( $R_{\text{int}} = 0.0568$ ), final  $R_1 = 0.0499$ ,  $wR_2 = 0.1215$ . Diffraction data were collected at 90 K on a Bruker SMART 1000 CCD diffractometer. Solution and refinement were solved by direct methods (standard SHELXS-97 package).

For **4**·3DMF,  $\text{Ni}_3\text{C}_{79}\text{H}_{103}\text{N}_{11}\text{O}_9\text{S}_4$ ,  $M = 1655.09$ , monoclinic, space group  $P2_1/c$ ,  $a = 17.009(3) \text{ \AA}$ ,  $b = 13.0882(16) \text{ \AA}$ ,  $c = 37.076(4) \text{ \AA}$ ,  $\alpha = 90^\circ$ ,  $\beta = 101.902(12)^\circ$ ,  $\gamma = 90^\circ$ ,  $V = 8076(9) \text{ \AA}^3$ ,  $Z = 4$ ,  $D_c = 1.361 \text{ Mg m}^{-3}$ ,  $\mu(\text{Cu-K}\alpha) = 2.277 \text{ mm}^{-1}$ ,  $T = 130(2)$ , crystal size,  $0.12 \times 0.10 \times 0.08 \text{ mm}^3$ , 16932 reflections measured, 10484 unique ( $R_{\text{int}} = 0.0487$ ), final  $R_1 = 0.0460$ ,  $wR_2 = 0.1013$ . Diffraction data were collected at 130 K on a Siemens P4 diffractometer. Solution and refinement were solved by direct methods (standard SHELXS-97 package).

- S. W. Ragsdale and M. Kumar, *Chem. Rev.*, 1996, **96**, 2515.
- T. I. Doukov, T. M. Iverson, J. Seravalli, S. W. Ragsdale and C. L. Drennan, *Science*, 2002, **298**, 567.
- C. Darnault, A. Volbeda, E. J. Kim, P. Legrand, X. Vernede, P. A. Lindahl and J.-C. Fontecilla-Camps, *Nat. Struct. Biol.*, 2003, **10**, 271.
- (a) J. Seravalli, Y. Xiao, W. Gu, S. P. Cramer, W. E. Antholine, V. Krymov, G. J. Gerfen and S. W. Ragsdale, *Biochemistry*, 2004, **43**, 3944; (b) M. A. Bramlett, X. Tan and P. A. Lindahl, *J. Am. Chem. Soc.*, 2003, **125**, 9316; (c) E. Webster, M. Y. Darensbourg, P. A. Lindahl and M. B. Hall, *J. Am. Chem. Soc.*, 2004, **126**, 3410; (d) R. P. Schenker and T. C. Brunold, *J. Am. Chem. Soc.*, 2003, **125**, 13962.
- (a) T. C. Harrop and P. K. Mascharak, *Acc. Chem. Res.*, 2004, **37**, 253; (b) P. K. Mascharak, *Coord. Chem. Rev.*, 2002, **225**, 201; (c) D. S. Marlin and P. K. Mascharak, *Chem. Soc. Rev.*, 2000, **29**, 69.
- T. C. Harrop, M. M. Olmstead and P. K. Mascharak, *Inorg. Chim. Acta*, 2002, **338**, 189.
- (a) R. Krishnan, J. K. Voo, C. G. Riordan, L. Zahkarov and A. L. Rheingold, *J. Am. Chem. Soc.*, 2003, **125**, 4422; (b) R. C. Linck, C. W. Spahn, T. R. Rauchfuss and S. R. Wilson, *J. Am. Chem. Soc.*, 2003, **125**, 8700; (c) M. L. Golden, M. V. Rampersad, J. H. Reibenspies and M. Y. Darensbourg, *Chem. Commun.*, 2003, 1824; (d) Q. Wang, A. J. Blake, E. S. Davies, E. J. L. McInnes, C. Wilson and M. Schröder, *Chem. Commun.*, 2003, 3012.
- J. Chen, S. Huang, J. Seravalli, H. Gutzman, Jr., D. J. Swartz, S. W. Ragsdale and K. A. Bagley, *Biochemistry*, 2003, **42**, 14822.
- (a) J. L. Craft, B. S. Mandimutsira, K. Fujita, C. G. Riordan and T. C. Brunold, *Inorg. Chem.*, 2003, **42**, 859; (b) G. Musie, P. J. Farmer, T. Tuntulani, J. H. Reibenspies and M. Y. Darensbourg, *Inorg. Chem.*, 1996, **35**, 2176.